

Stress determination through diffraction: establishing the link between Kröner and Voigt/Reuss limits

Conal E. Murray,^{1,a)} Jean L. Jordan-Sweet,¹ Stephen W. Bedell,¹ and E. Todd Ryan²

¹IBM T.J. Watson Research Center, Yorktown Heights, New York 10598

²GLOBALFOUNDRIES Inc., Albany, New York 12203

(Received 9 March 2015; accepted 12 March 2015)

The quantification of stress in polycrystalline materials by diffraction-based methods relies on the proper choice of grain interaction model that links the observed strain to the elastic stress state in the aggregate. X-ray elastic constants (XEC) relate the strain as measured using X-rays to the state of stress in a quasi-isotropic ensemble of grains. However, the corresponding interaction models (e.g., Voigt and Reuss limits) often possess unlikely assumptions as to mechanical response of the individual grains. The Kröner limit, which employs a self-consistent scheme based on the Eshelby inclusion method, is based on a more physical representation of isotropic grain interaction. For polycrystalline aggregates composed of crystals with cubic symmetry, Kröner limit XEC are equal to those calculated from a linear combination of Reuss and Voigt XEC, where the weighting fraction, x_{Kr} , is solely a function of the single-crystal elastic constants and scales with the material's elastic anisotropy. This weighting fraction can also be experimentally determined using a linear, least-squares regression of diffraction data from multiple reflections. Data on metallic thin films reveals that this optimal experimental weighting fraction, x^* , can vary significantly from x_{Kr} , as well as that of the Neerfeld limit ($x=0.5$). © 2015 International Centre for Diffraction Data. [doi:10.1017/S0885715615000238]

Key words: stress determination, polycrystalline materials, x-ray diffraction, strain anisotropy, elasticity

I. INTRODUCTION

During the past century, X-ray diffraction has been used to probe the crystalline structure of materials, where detecting the change in lattice spacing as a function of orientation allows for the determination of strain in reciprocal space. However, the quantification of stress in materials using X-ray diffraction relies on the proper use of X-ray elastic constants (XEC). XEC are required to extract stress from the measured strains due to the effects of strain anisotropy, which results from the fact that the elastic response of the diffracting grains varies in the case of polycrystalline ensembles composed of elastically anisotropic grains. An example of this effect is illustrated in Figure 1, where the normalized lattice spacings of a 6 μm thick sputtered Ni film on a Si (111) substrate were measured for four different (hkl) reflections as a function of $\sin^2(\psi)$, with ψ defined as the angle between the sample surface normal and the diffraction vector. For quasi-isotropic polycrystalline aggregates, the ratio of the fitted slopes, m , of the d vs. $\sin^2(\psi)$ data to the unstressed lattice spacings, d_0 , is proportional to the in-plane stress in materials [see Eq. (3)] with no finite out-of-plane components of the film's stress tensor (Noyan and Cohen, 1987). Under the assumption that the in-plane, residual stress in the Ni film is equal for all grains, then the XEC must clearly differ for these reflections. In fact, Table 1, which lists these ratios, indicates that the use of a single value of

XEC for all reflections would result in a variation of 73% in the resulting in-plane stress.

Given this large discrepancy, it is important to determine the correct forms of XEC that provide the most consistent depiction of elastic behavior based on X-ray diffraction measurements conducted over multiple reflections. Section II describes the various grain interaction models and the methodologies associated with diffraction-based stress analysis. The experimental details are contained in Section III followed by a discussion of the results in Section IV. The conclusions are summarized in Section V.

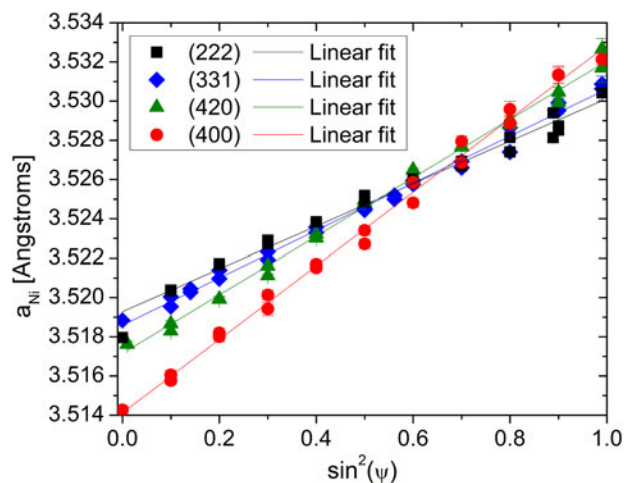


Figure 1. (Color online) Measurements of normalized lattice spacing ($a = d_{hkl}\sqrt{h^2 + k^2 + l^2}$) as a function of $\sin^2(\psi)$ and corresponding linear fits of a 6 μm thick Ni film for four different reflections.

^{a)}Author to whom correspondence should be addressed. Electronic mail: conal@us.ibm.com

TABLE I. Ratio of fitted slope to intercept (m/d_0) as calculated from d vs. $\sin^2(\psi)$ analyses from multiple (hkl) reflections of a $6\ \mu\text{m}$ thick Ni film and their relative difference from the (222) data

Ni	m/d_0	Normalized difference
(222)	0.00308(9)	1
(331)	0.00342(6)	1.110
(420)	0.00423(6)	1.373
(400)	0.00533(9)	1.731

II. STRESS DETERMINATION USING DIFFRACTION

For a quasi-isotropic ensemble of crystals, the strain as measured using diffraction is related to the volume-averaged stress tensor, $\bar{\sigma}_{ij}$, through the traditional X-ray stress/strain equation (Stickforth, 1966):

$$\langle \varepsilon_{33}^L \rangle = S_1^{\text{XEC}} \bar{\sigma}_{ii}^S + \frac{1}{2} S_2^{\text{XEC}} a_{3m}^{\text{LS}} a_{3n}^{\text{LS}} \bar{\sigma}_{mn}^S \quad (1)$$

where S_1^{XEC} and $(1/2)S_2^{\text{XEC}}$ represent the XEC and a_{ij}^{LS} the direction cosines associated with the transformation from the sample coordinate system to the laboratory coordinate system. Let us simplify Eq. (1) to the case of isotropic, in-plane biaxial stress ($\sigma_{11} = \sigma_{22} = \sigma_0^S$) with all other components of the stress tensor being equal to zero, corresponding to the stress state of a blanket thin film.

$$\langle \varepsilon_{33}^L \rangle = \frac{d_{hkl} - d_0}{d_0} = \sigma_0^S [2S_1^{\text{XEC}} + \frac{1}{2} S_2^{\text{XEC}} \sin^2(\psi)] \quad (2)$$

where d_0 refers to the unstrained lattice spacing of the material. By taking the derivative of Eq. (2) with respect to $\sin^2(\psi)$:

$$\frac{1}{d_0} \frac{\partial d_{hkl}}{\partial \sin^2(\psi)} = \left(\frac{m}{d_0} \right)_{hkl} = \frac{1}{2} S_2^{\text{XEC}} \sigma_0^S \quad (3)$$

where m is the slope of a linear fit of the d vs. $\sin^2(\psi)$ plot for a particular (hkl).

Establishing the specific XEC values depends on the nature of the specimen under investigation. For single-crystal samples, a unique correspondence exists between elastic stress and strain, as defined by the compliance or stiffness tensors, C_{ijkl}^C or S_{ijkl}^C , respectively. For polycrystalline aggregates, assumptions regarding the mechanical behavior within the grains are necessary. For polycrystalline aggregates composed of crystals possessing cubic symmetry, Reuss-averaged XEC, which assume that the stress tensors of the constituent crystals are all equivalent, can be represented as (Reuss, 1929), (Möller and Martin, 1939), and (Stickforth, 1966):

$$S_1^{\text{R}} = S_{1122}^{\text{C}} + S_0 \Gamma \quad \text{and} \quad \frac{1}{2} S_2^{\text{R}} = S_{1111}^{\text{C}} - S_{1122}^{\text{C}} - 3S_0 \Gamma \quad (4)$$

where S_{ijkl}^{C} represent the single-crystal compliance tensor coefficients and $S_0 = S_{1111}^{\text{C}} - S_{1122}^{\text{C}} - 2S_{1212}^{\text{C}}$. The orientation parameter, Γ , is a function of the Miller indices of the reflection under investigation (hkl):

$$\Gamma = \frac{h^2 k^2 + h^2 l^2 + k^2 l^2}{(h^2 + k^2 + l^2)^2} \quad (5)$$

The Voigt-limit XEC, which assume that the crystallite strain tensors are equal, take the form (Voigt, 1928):

$$S_1^{\text{V}} = \frac{S_0(S_{1111}^{\text{C}} + 2S_{1122}^{\text{C}}) + 10S_{1222}^{\text{C}} S_{1212}^{\text{C}}}{3S_{1111}^{\text{C}} - 3S_{1122}^{\text{C}} + 4S_{1212}^{\text{C}}}, \quad (6)$$

$$\frac{1}{2} S_2^{\text{V}} = \frac{10S_{1212}^{\text{C}}(S_{1111}^{\text{C}} - S_{1122}^{\text{C}})}{3S_{1111}^{\text{C}} - 3S_{1122}^{\text{C}} + 4S_{1212}^{\text{C}}}$$

Although the assumptions associated with the Voigt and Reuss models are not representative of the actual mechanical behavior in a polycrystalline aggregate, they represent upper and lower bounds, respectively, on the elastic strain energy generated within such an ensemble (Hill, 1952). The mechanical behavior of the entire aggregate can be represented by a linear combination of these limits to generate a weighted XEC model (Serruys *et al.*, 1988), (Van Houtte and De Buyser, 1993):

$$S_1^{\text{W}} = S_1^{\text{V}}(1-x) + xS_1^{\text{R}}, \quad \frac{1}{2} S_2^{\text{W}} = \frac{1}{2} S_2^{\text{V}}(1-x) + x\frac{1}{2} S_2^{\text{R}} \quad (7)$$

The Neerfeld limit (Neerfeld, 1942) corresponds to an arithmetic average of the Voigt and Reuss limits, where $x = 0.5$.

Under the Kröner limit, the elastic anisotropy of the crystallite is incorporated into an elastic susceptibility tensor, t_{ijkl} , while the aggregate is represented by an elastically isotropic matrix, S_{ijkl}^{B} (Eshelby, 1957), (Kröner, 1958). For a polycrystalline aggregate composed of cubic crystals, the XEC take the form (Bollenrath *et al.*, 1967), (Dölle, 1979):

$$S_1^{\text{K}} = S_{1122}^{\text{B}} + t_1 + t_0 \Gamma, \quad (8)$$

$$\frac{1}{2} S_2^{\text{K}} = 2S_{1212}^{\text{B}} + 2t_2 + t_0(1-3\Gamma)$$

where $t_0 = t_{1111} - t_{1122} - 2t_{1212}$, $t_1 = t_{1122}$, $t_2 = t_{1212}$. For quasi-isotropic aggregates composed of crystals with hexagonal symmetry, Voigt limit XEC are contained in (Behnken and Hauk, 1986); (Van Houtte and De Buyser, 1993), (Murray, 2013) for the Reuss limit, and (Behnken and Hauk, 1986), (Tanaka *et al.*, 2000), and (Murray, 2013) under the Kröner limit.

The question arises as to whether a relationship can be derived between the XEC associated with the Voigt and Reuss limits and those under the Kröner limit, which represents a more realistic depiction of the mechanical response of a polycrystalline aggregate. Since the traditional Voigt limit XEC are constant for a given material, direct inspection of the terms in Eqs (4), (7), and (8) that depend on Γ shows that the following weighting fraction, x_{Kr} , equates the Kröner and weighted Voigt/Reuss limit XEC:

$$x_{\text{Kr}} = \frac{t_0}{S_0} \quad (9)$$

In fact, it has been proven that for cubic materials a single value of the weighting fraction satisfies this relation for all reflections of a polycrystalline aggregate (Murray, 2013). Table II contains values of the elastic constant parameters S_{ijkl} , t_{ijkl} and the corresponding x_{Kr} and Zener anisotropic factor, $A = 2(S_{1111}^{\text{C}} - S_{1122}^{\text{C}})/4S_{1212}^{\text{C}}$ for cubic materials. As can be observed, t_0 values decrease monotonically with A since the

TABLE II. Single-crystal stiffness tensor coefficients (S_{ijkl}^C), corresponding Kröner compliance (S_{ijkl}^B), and susceptibility tensor (t_{ijkl}) components, Zener anisotropy ratios, A , and corresponding x_{Kr} values for a variety of materials (units for S_{ijkl} and t_{ijkl} are in TPa^{-1} , A and x_{Kr} are unitless).

	S_{1111}^C	S_{1122}^C	S_{1212}^C	S_{1212}^B	t_{1212}	t_0	A	x_{Kr}
Cu	15.0	-6.28	3.32	5.19	-1.08	5.39	3.20	0.368
Ni	7.34	-2.74	2.00	2.87	-0.50	2.48	2.52	0.408
Fe	7.59	-2.83	2.16	3.05	-0.50	2.51	2.41	0.411
Al	15.7	-5.66	8.77	9.49	-0.35	1.73	1.22	0.452
W	2.57	-0.73	1.65	1.65	0	0	1	0.48

elastic susceptibility tensor is a function of the elastic anisotropy of the constituent crystallites that comprise the polycrystalline aggregate. However, x_{Kr} increases with decreasing A , indicating that S_0 decreases more rapidly than t_0 as the material's elastic anisotropy approaches 1. In the limiting case of elastically isotropic crystallites ($A = 1$), both t_0 and S_0 are zero. However, as shown in Table II, W possesses a finite value of $x_{Kr} = 0.48$. By analyzing the full form of the quotient t_0/S_0 , we can derive the limit to which x_{Kr} converges for $A = 1$ based on the single-crystal constants. From Murray (2013), the full form of x_{Kr} can be expressed as:

$$x_{Kr} = \frac{2w_2 C_2 C_2^B (C_0 + 2C_2)}{C_2^B (C_2 - C_2^B + 2w_2 C_2^B) (C_0 + 2C_2 - 2C_2^B + 4w_2 C_2^B)} \quad (10)$$

where $C_2 = C_{1212}^C$, $C_0 = C_{1111}^C - C_{1122}^C - 2C_{1212}^C$ and C_2^B corresponds to the second stiffness tensor coefficient calculated under the Kröner limit for the elastically isotropic matrix. w_2 represents the second coefficient of the inverse of the Eshelby tensor for spherical inclusions:

$$w_2 = \frac{5(C_0 + 3C_1 + 2C_2 + 4C_2^B)}{4(C_0 + 3C_1 + 2C_2 + 6C_2^B)} \quad (11)$$

with $C_1 = C_{1122}^C$. For elastically isotropic crystallites, C_0 is zero and $C_2 = C_2^B$, allowing Eq. (10) to be simplified:

$$\lim_{C_0 \rightarrow 0} x_{Kr} = \frac{1}{2w_2} = \frac{8}{15} - \frac{2}{15} \frac{C_{1122}^C}{C_{1111}^C} \quad (12)$$

It is of interest to note that, although this limit can vary as a function of the single-crystal elastic constants, the value for W (0.48) coincides with that produced by a linear fitting of 44 types of materials possessing cubic symmetry (Murray, 2013).

In order to assimilate data obtained by X-ray measurements from multiple reflections, we create a procedure based on a least-squares determination of the X-ray stress/strain equation [Eq. (2)]. From the weighted Voigt-Reuss XEC of Eq. (7), we can rewrite Eq. (3):

$$\left(\frac{m}{d_0}\right)_{hkl} = (a_{hkl}x + b)\sigma_0^S = a_{hkl}y + b\sigma_0^S \quad (13)$$

where $a_{hkl} = (1/2)S_2^R - (1/2)S_2^V$ is a coefficient that varies with (hkl) , $b = (1/2)S_2^V$ is constant for each material and $y = x\sigma_0^S$ is a secondary variable. To determine the optimal values of σ_0^S and $x^* = y/\sigma_0^S$, we minimize the residual error for fits performed on n reflections (Murray *et al.*, 2013). Note that this procedure can be applied to polycrystalline

aggregates with crystals possessing any symmetry (not just cubic) so long as the ensemble can be treated as quasi-isotropic.

III. EXPERIMENTAL DETAILS

The residual stress within three types of thin films was investigated using X-ray diffraction. The $0.5 \mu\text{m}$ thick Ti films were sputter deposited onto oxidized, 300 mm diameter Si (001) substrates and capped with a 5 nm thick TiN layer. $0.9 \mu\text{m}$ thick Cu films were electroplated onto sputter deposited TaN/Ta/Cu seed layers, also on oxidized, 300 mm diameter Si (001) substrates. The $6 \mu\text{m}$ thick Ni films were deposited onto 100 mm diameter Si (111) substrates using DC magnetron sputtering at 1 kW power and 10 mTorr Ar pressure. Diffraction measurements were conducted at Brookhaven National Laboratory's National Synchrotron Light Source X20A beamline. Measurements conducted on the Ni films were performed using a photon energy of 11.2 keV, while those on the Cu and Ti films used a photon energy of 8.6 keV. Diffractive optics consisted of a double-crystal Ge (111) monochromator and a single-bounce Ge (111) analyzer crystal, in non-dispersive configuration with the sample. The angular width of the incident beam at the detector was measured to be 0.012° full width at half maximum (FWHM) in the diffraction plane.

Conventional d vs. $\sin^2(\psi)$ measurements were conducted on a number of reflections for the three films. Twenty-one points were taken in positive and negative ψ tilts corresponding to a range of $\sin^2(\psi)$ from 0 to 0.99. Lorentzian fits were performed on the diffraction data to determine peak centers, from which lattice spacing values were calculated using Bragg's law. Four reflections were used for the Ni films: (400), (420), (331), (222); and (200), (220), (311), and (222) for the Cu films, spanning the allowable range of Γ from 0 to 1/3. Six reflections for the Ti films were used: (0004), (10 $\bar{1}$ 4), (2022), (20 $\bar{2}$ 2), (11 $\bar{2}$ 0), and (2020), which span the comparable range of orientation for hexagonal crystals. XEC values were calculated using single crystal stiffness tensor components from Simmons and Wang (1971) and lattice parameter values from Wood (1962) for the case of the hexagonal Ti film. A secondary piece of the Ti film was thermally cycled to 400 °C for 30 s to assess the effects of heat treatment.

IV. RESULTS AND DISCUSSION

The curves corresponding to in-plane stress values, calculated as a function of the weighting fraction, x , are depicted in Figures 2(a), 2(b), and 3 for the Ni, Ti, and Cu films, respectively, along with the least-squares fitted values among all of the measured reflections. Figure 2(a) indicates that the Ni film

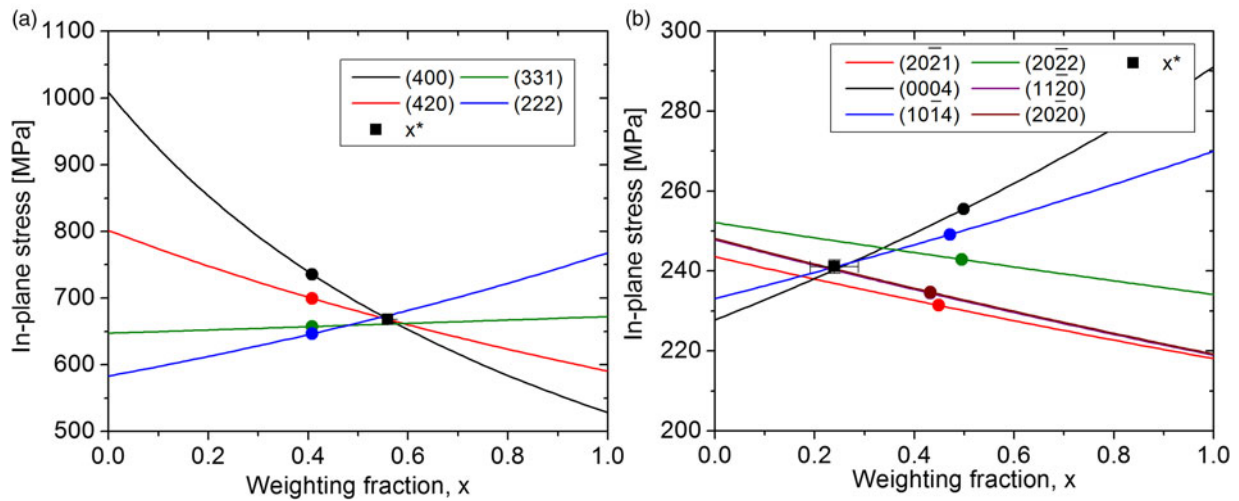


Figure 2. (Color online) Plot of in-plane stress as calculated from X-ray diffraction reflections of a (a) 6 μm thick Ni film and (b) 0.5 μm thick Ti film as a function of x , the Voigt–Reuss weighting fraction. The circles correspond to values computed using XEC under the Kröner limit, x_{Kr} , and the square value determined by least-squares fitting, x^* .

exhibits an optimal weighting fraction value, $x^* = 0.56 \pm 0.01$, that is closer to the Neerfeld limit (0.5) than that corresponding to the Kröner limit ($x_{\text{Kr}} = 0.408$) in Table II. This value of x^* results in an effective value of $\frac{1}{2} S_2$ for the Ni (420) reflection (6.338 TPa^{-1}) that closely matches the experimental value of 6.32 TPa^{-1} as determined by Macherauch (1966). In contrast, Figure 2(b) indicates that the Ti film possesses an optimal weighting fraction of 0.24 ± 0.05 , which is significantly below the Neerfeld limit (0.5) as well as those corresponding to the Kröner limit, which are not constant for hexagonal crystals but vary from 0.43 to 0.5 depending on the reflection (Murray, 2013). However, the fact that the curves nearly coincide for the (11 $\bar{2}$ 0) and (20 $\bar{2}$ 0) reflections confirms that the Ti film behaves as a quasi-isotropic, polycrystalline aggregate. For the Ti film subject to the 400 °C anneal, a weighting fraction of 0.27 ± 0.05 was obtained, overlapping the x^* value for the unannealed Ti film within experimental error.

The optimal XEC weighting fraction for the Cu film (0.62 ± 0.06), as shown in Figure 3(a), is greater than the Kröner

value ($x_{\text{Kr}} = 0.368$) and consequently closer to the Neerfeld fraction (0.5). Figure 3(b) illustrates that the use of x^* to ascertain in-plane stress clearly produces values that are more consistent ($198 \pm 8 \text{ MPa}$) than either those associated with Kröner limit ($199 \pm 11 \text{ MPa}$) or Neerfeld limit ($207 \pm 24 \text{ MPa}$) XEC. Measurements conducted on multiple Cu thin-film samples exhibit x^* values that range from approximately 0.5–0.7 (Murray *et al.*, 2013) with no clear trend with respect to thickness. Since these films experienced different thermal treatments, it is possible that the degree of plastic relaxation within the Cu sample is responsible for this variation.

In fact, plastic deformation has been noted to have a large impact on XEC weighting fraction values (Macherauch, 1966). Since the Ti unit cell has fewer available slip systems than the FCC unit cells associated with Ni and Cu, the minor change in x^* observed due to thermal cycling of the Ti film may be an effect of the limited plastic deformation during a thermal excursion to 400 °C. These experiments also demonstrate that film thickness does not correlate with x^* ,

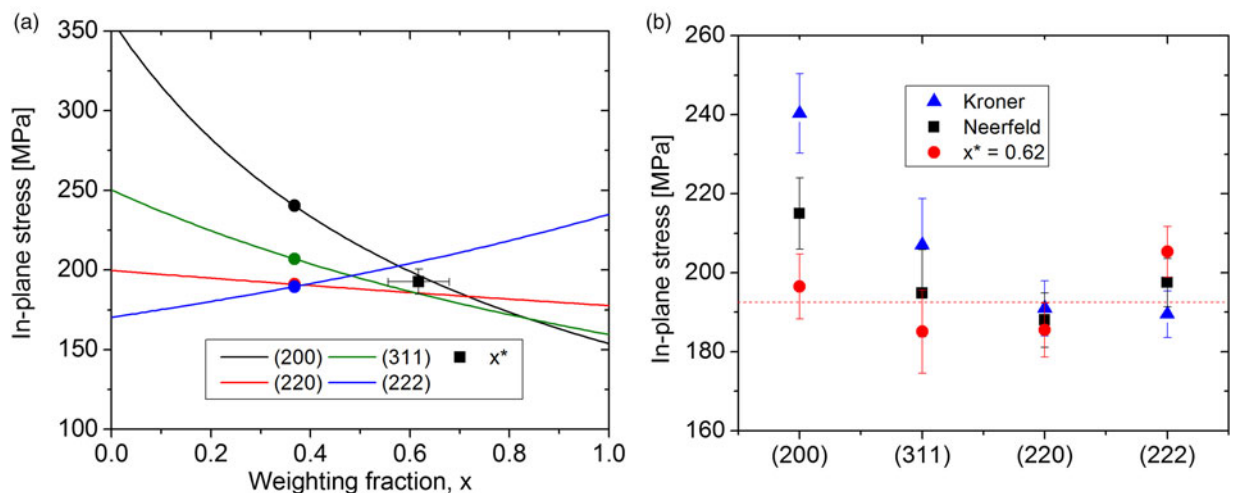


Figure 3. (Color online) (a) Plot of in-plane stress as calculated from four different X-ray diffraction reflections of a 0.9 μm thick Cu film as a function of x , the Voigt–Reuss weighting fraction. The circles correspond to values computed using XEC under the Kröner limit, x_{Kr} , and the square value determined by least-squares fitting, x^* . (b) Comparison of in-plane stress values determined from XEC calculated under the Kröner limit, Neerfeld limit and using x^* , where the dotted red line represents the optimized in-plane stress (198 MPa).

since the Cu film ($0.9\ \mu\text{m}$) exhibits x^* values that are larger than those of the Ti films ($0.5\ \mu\text{m}$) as well as the Ni film ($6\ \mu\text{m}$), so that many factors may be responsible in dictating the XEC weighting fraction.

V. CONCLUSIONS

In comparing grain interaction models necessary to convert X-ray diffraction data into stress values, the effects of strain anisotropy necessitate the use of XEC that depend on the X-ray reflection under investigation and are not equal to the bulk elastic constants of the material. The Kröner limit XEC were found to be equivalent to a weighted Voigt/Reuss approach for polycrystalline aggregates displaying cubic symmetry. However, experimental results from measurements performed on Cu, Ni, and Ti thin films reveal that the optimal Voigt/Reuss weighting fractions, x^* , as determined from least-squares fitting over multiple X-ray reflections, can substantially differ from both the Neerfeld model ($x = 0.5$) and the Kröner model. The use of x^* results in residual, in-plane stress values that are more consistent than those produced using either Neerfeld or Kröner XEC.

ACKNOWLEDGMENTS

This work was performed by the Research Alliance Teams at various IBM Research and Development facilities. Use of the National Synchrotron Light Source, Brookhaven National Laboratory, was supported by the U.S. Department of Energy, Office of Science, Office of Basic Energy Sciences under Contract No. DE-AC02-98CH10886.

- Behnken, H. and Hauk, V. (1986). "Berechnung der Röntgenographischen Elastizitätskonstanten (REK) des Vielkristalls aus den Einkristalldaten für beliebige Kristallsymmetrie," *Z. Metallk.* **77**, 620–626.
- Bollenrath, F., Hauk, V. and Müller, E. H. (1967). "Zur Berechnung der vielkristallinen Elastizitätskonstanten aus den Werten der Einkristalle," *Z. Metallk.* **58**, 76–82.

- Dölle, H. (1979). "The influence of multiaxial stress states, stress gradients and elastic anisotropy on the evaluation of (residual) stresses by x-rays," *J. Appl. Crystallogr.* **12**, 489–501.
- Eshelby, J. D. (1957). "The determination of the elastic field of an ellipsoidal inclusion, and related problems," *Proc. R. Soc. Lond. A* **241**, 376–396.
- Hill, R. (1952). "The elastic behaviour of a crystalline aggregate," *Proc. Phys. Soc. A* **65**, 349–354.
- Kröner, E. (1958). "Berechnung der elastischen Konstanten des Vielkristalls aus den Konstanten des Einkristalls," *Z. Phys.* **151**, 504–518.
- Macherauch, E. (1966). "X-ray stress analysis," *Exp. Mech.* **6**, 140–153.
- Möller, H. and Martin, G. (1939). "Elastische Anisotropie und röntgenographische Spannungsmessung," *Mitt. Kaiser-Wilhelm-Inst. Eisenforsch. Düsseldorf* **21**, 261–269.
- Murray, C. E. (2013). "Equivalence of Kröner and weighted Voigt–Reuss models for x-ray stress determination," *J. Appl. Phys.* **113**, 153509.
- Murray, C. E., Bedell, S. W. and Ryan, E. T. (2013). "Weighted mechanical models for residual stress determination using x-ray diffraction," *J. Appl. Phys.* **114**, 033518.
- Neerfeld, H. (1942). "Zur Spannungsberechnung aus röntgenographischen Dehnungsmessungen," *Mitt. K.-Wilh.-Inst. Eisenforsch.* **24**, 61–70.
- Noyan, I. C. and Cohen, J. B. (1987). "*Residual Stress*" (Springer-Verlag, NY).
- Reuss, A. (1929). "Berechnung der Fließgrenze von Mischkristallen auf Grund der Plastizitätsbedingung für Einkristalle," *Z. Agnew. Math. Mech.* **9**, 49–58.
- Serruys, W., Van Houtte, P. and Aermoudt, E. (1988). "Why are X-ray measurements different from mechanical residual stress measurements?" *Manuf. Technol.* **37**, 527–530.
- Simmons, G. and Wang, H. (1971). "*Single Crystal Elastic Constants and Calculated Aggregate Properties*" (MIT Press, MA).
- Stickforth, J. (1966). "Über den Zusammenhang zwischen röntgenographischer Gitterdehnung und makroskopischen elastischen Spannungen," *Tech. Mitt. Krupp Forsch. Ber.* **24**, 89–102.
- Tanaka, K., Suzuki, K., Sakaida, Y., Kimachi, H. and Akiniwa, Y. (2000). "Single crystal elastic constants of β -Silicon Nitride determined by X-ray powder diffraction," *Mater. Sci. Res. Int.* **6**, 249–254.
- Van Houtte, P. and De Buyser, L. (1993). "The influence of crystallographic texture on diffraction measurements of residual stress," *Acta Metall. Mater.* **41**, 323–336.
- Voigt, W. (1928). *Lehrbuch der Kristallphysik* (Teubner, Leipzig).
- Wood, R. M. (1962). "The lattice constants of high purity alpha titanium," *Proc. Phys. Soc.* **80**, 783–786.